VVER-1000 Weapons-Grade MOX Computational Benchmark Analysis

M. A. Kalugin and A. P. Lazarenko
Russian Research Center – "Kurchatov Institute"
Moscow, Russia
kalugin@adis.vver.kiae.ru; laz@vver.kiae.ru

A. G. Kalashnikov
Institute of Physics and Power Engineering
Obninsk, Russia
moseev@ippe.rssi.ru

J. C. Gehin
Oak Ridge National Laboratory
Oak Ridge, TN, USA 37831-6363
gehinjc@ornl.gov

ABSTRACT

Calculations of computational benchmark problems for the disposition of weapons-grade plutonium fuel in VVER-1000 reactors have been performed under the Joint U.S./Russian Fissile Material Disposition Program. The benchmarks cover pin cell, single fuel assembly, and multi-assembly structures with several different fuel types, moderator densities, and boron content for operational and off-normal conditions. Fuel depletion is performed to a burnup of 60 MWd/kgHM. The results of the analysis of the benchmarks with U.S. and Russian code systems have been compared and indicated good agreement among the different methods and data.

1. INTRODUCTION

Within the framework of Joint United States/Russian Fissile Materials Disposition Program an important task is to verify and validate computer codes for the use of MOX fuel in VVER-1000 reactors. Benchmark analyses are being performed for both computational benchmarks and experimental benchmarks. The goal of the computational benchmarks is a direct comparison of the methods in use at Oak Ridge National Laboratory (ORNL) with those used in Russia at the Russian Research Center – "Kurchatov Institute" (RRC-KI) in Moscow and the Institute of Physics and Power Engineering (IPPE) in Obninsk.

The computational benchmarks consist of 18 calculational variants of VVER-1000 pin cells, single fuel assemblies, and multiple fuel assemblies. Each variant has various numbers of

calculational states representing different operating conditions (both normal and off-normal). Several of the benchmarks also include fuel depletion. The primary quantities of interest are the effective multiplication factor (k_{eff}), reaction rates, neutron fluxes, nuclide densities, and kinetics parameters. The primary fuel of interest is weapons-grade (WG) mixed-oxide (MOX) fuel, but variants containing UO_2 and reactor-grade (RG) MOX were also investigated. Preliminary results for this series of benchmarks were previously reported in Refs. 1–3.

2. BENCHMARK DESCRIPTION

Two sets of benchmark variants were formulated by the Russian participants in the Joint United States/Russian Federation Plutonium Disposition Program. The first set[4] covered different aspects of UO_2 and MOX in VVER-1000 reactors in normal operating conditions. The second set[5] was formulated to cover off-normal conditions and provide for a comparison of kinetics parameters. The complete specifications of the benchmarks are available in Ref. 6.

The benchmarks consist of a series of 20 variants, described in Table 1, which differ in geometry and fuel composition. Each variant is calculated under various conditions as indicated by different states, described in Table 2. The first set of variants (V1-V14) use the states typical of standard operating conditions (S1-S6), while the second set of variants (V15-V20) use the states indicative of off-normal and accident conditions (S7-S12). Fuel burnup, however, is performed only under state 1 to an average burnup of 60 MWd/kgHM. The power density for the burnup calculations is 108 MW/m^3, which is typical of operating VVER-1000 reactors.

The benchmark geometries consist of a pin cell, a standard VVER-1000 assembly, and a multi-assembly structure formed by two different assembly types. The pin cell cases represent a VVER-1000 fuel pin in an infinite triangular lattice with a pitch of 1.275 cm. The fuel pin consists of a 0.772-cm diameter fuel pellet and zirconium cladding with a thickness of 0.0722 cm. The VVER-1000 assembly configuration, shown in Fig. 1, contains fuel rods, guide tubes, and a central instrument tube. In this figure, the fuel is indicated as cell types 1, 4, and 5, the guide tubes are indicated as cell type 3, and the central instrument tube is indicated as cell type 2. The different fuel cell types indicate regions with possible different plutonium loadings allowing a graded-assembly design. The final geometry considered is that of the multi-assembly structure show in Fig. 2. This structure consists of an infinite lattice of two assembly types K1 (MOX) and K2 (UO_2) resulting in a MOX to UO_2 ratio of 1:3. This structure allows the investigation of the MOX and UO_2 interface.

Several different fuel materials were considered in the benchmarking activity, including fresh UO_2, fresh WG MOX(93 wt.% ^{239}Pu, 5 wt.% ^{240}Pu, 1 wt.% ^{241}Pu), fresh RG MOX(62 wt.% ^{239}Pu, 27 wt. % ^{240}Pu, 6 wt. % ^{241}Pu, 5 wt. % ^{242}Pu), spent UO_2, spent WG MOX, and fresh MOX with individual plutonium isotopes. The fresh WG MOX has different plutonium content for graded fuel designs (ranging from 2.2 wt. % to 4.7 wt. % Pu). The cladding, guide tube, and instrument tube material is zirconium. The control rods indicated in state 2 use B_4C as the absorber material. All depletions are performed with a natural boron concentration of 600 ppm by weight (0.6 g B/kg H_2O).

The calculational results requested in the benchmark include k_{eff}, migration area, concentration of major actinides and fission products, pin-by-pin power (fission) distributions, neutron fluxes,

one-group macroscopic cross sections, and kinetics parameters. A comparison of a subset of all of these results is given in Section 4.

3. CALCULATIONAL METHODS

Calculations of the different benchmark variants were performed using the MCU, CONKEMO, TVS-M, TRIANG-PWR, WIMS-ABBN, and HELIOS code systems. A brief description of each code is given below:

MCU-RFFI/A – Continuous energy Monte Carlo code[7] developed at RRC-KI. The code system also has the ability to use group cross sections. Recently MCU-RFFI/A has been combined with a burnup module to allow fuel depletion calculations.

CONKEMO – KENO Multi-group Monte Carlo code[8] with cross sections based on IPPE nuclear data[9] combined with ORIGEN code for depletion calculations. This code system is under development at IPPE.

TVS-M – Spectral code for VVER lattice and assembly burnup calculations[10] developed at RRC-KI using nuclear data library obtained from the same source as MCU-RFFI/A code. The library has 48 energy groups with 24 thermal groups.

TRIANG-PWR – Diffusion-theory-based code[4] for pin-by-pin computation using constants from WIMS-ABBN (IPPE).

WIMS-ABBN – An updated version of the WIMS-D4 code[11] in which minor actinide chains have been added and the cross section library has been updated. The WIMS-ABBN library is based on the FOND-2 evaluated nuclear data files and has 69 energy groups.

HELIOS – Fuel assembly code system[12] (developed by Studsvik Scandpower Inc.). The calculations were performed using the HELIOS version 1.4 with ENDF/B-VI-based 190-group cross section library.

VENTURE – Finite-difference diffusion theory code system[13] developed at ORNL. In the benchmark analysis this code system used only for the calculation of kinetics parameters (effective delayed neutron fraction and prompt neutron life time) using homogenized cross sections obtained from HELIOS.

As the above code descriptions indicate, there are two Monte Carlo methods, three integral transport methods, and two diffusion-theory-based methods. Three distinct sets of data are used by the various codes.

4. RESULTS

The complete calculational results for the benchmarks are given in Refs. 4 and 6. In addition to the results presented, calculations of the pin-cell variants with the SAS2H module of SCALE have also been completed and are available in Ref. 14. A subset of key results will be presented for the pin cell variants, assembly variants, and multi-assembly variants. In most cases, TVS-M was arbitrarily chosen as the reference.

4.1 PIN CELL RESULTS

A comparison of the k_{eff} results for the pin cell variants 1-4, 7-10 are given in Table 3 in terms of percent difference from the TVS-M values. The results show good agreement for nearly all cases with differences generally below 0.5% between TVS-M, MCU, and HELIOS. The WIMS-ABBN results show slightly larger deviations from TVS-M with maximum differences of over 1%. The best agreement occurs for fresh UO_2 fuel and the difference increases for MOX and for spent fuel. The comparison of the multiplication factors computed with the individual isotopes (V7-V9) show good agreement for ^{239}Pu and ^{240}Pu. The differences in k_{eff} for the ^{241}Pu variant (V9) are substantially larger with TVS-M and MCU agreeing well, but differing by approximately 3% from HELIOS and WIMS-ABBN. Recall that TVS-M and MCU use a common data source, which explains the agreement between these codes. The multiplication factors for the other pin cell variants V15-V18, which are not presented, show similar agreement.

The multiplication factors for pin cell variants V1-V4, and V10 were used to compute reactivity effects of the fuel temperature (Doppler), boron concentration, fission product poisoning (^{135}Xe and ^{149}Sm), and total temperature (isothermal). A comparison of the reactivity effects with respect to the TVS-M results for the 0 MWd/kg burnup point are given in Fig. 3. The results show generally good agreement with two exceptions: WIMS-ABBN shows large differences with respect to the temperature effects and TVS-M appears to be over-estimating the fission product poisoning relative to the other codes. The reactivity effects for the off-normal conditions are shown in Fig. 4 for fuel temperature change, boron concentration, and coolant voiding. The results generally indicate good agreement.

Burnup calculations were performed for pin cell variants 1,2 and 10. A comparison of the results is presented in Figs. 5, 6, and 7 for these variants. The comparison of the UO_2 burnup results indicate the k_{eff} values to be within ±0.6% over the 60 MWd/kgHM depletion. The WG MOX comparison (V2) show a larger discrepancy with the HELIOS and WIMS-ABBN showing similar trends in k_{eff} but differing from the TVS-M values by more than 1% at 60 MWd/kg. The results for the RG MOX (V10) are similar with HELIOS and WIMS-ABBN showing similar trends but differing from TVS-M by 1.5-2.0% at 60 MWd/kgHM.

4.2 SINGLE ASSEMBLY RESULTS

A comparison of the k_{eff} values for the UO_2 (V11) and uniform WG-MOX (V12) variants are presented in Table 4 for the various states at 0 and 60 MWd/kgHM. The results show generally good agreement with the differences for UO_2 fuel not exceeding 1% and WG MOX fuel not exceeding 1.2% at 0 MWd/kg. The differences are somewhat larger at 60 MWd/kg burnup, ranging from 1–2%. The reactivity effects are shown in Fig. 3 demonstrate good agreement with the differences not exceeding 5% in the UO_2 assembly and 10% in the WG MOX assembly. The

only exception is WIMS-ABBN, which overestimates the Doppler effect and total temperature effect in comparison to the other codes. The control rod worth was also computed using the state 1 and 2 k_{eff} values. The results, which are presented in Table 5, show very good agreement.

The comparison of the k_{eff} values versus burnup is presented in Fig. 8 and show similar trends as the pin cell variants. The differences lie within ±0.7% for UO_2 and ±1.5% for WG MOX fuel. Again, the WIMS-ABBN and HELIOS results show a similar trend for the WG MOX case.

The pin-by-pin power distributions were compared for all of the codes and are in good agreement. TVS-M slightly under-estimates the power values in the boundary pins. However, the maximum differences between all calculations do not exceed 5%.

4.3 MULTI-ASSEMBLY STRUCTURE

Calculations of the burnup of the multi-assembly structures with UO_2 and uniform WG MOX (V13) and graded WG MOX (V14) assemblies were performed with TVS-M, CONKEMO, and HELIOS. A comparison of the k_{eff} values as a function of burnup is given in Fig. 9. The results show good agreement with k_{eff} generally agreeing within ±1 %. Comparisons of the pin-by-pin power distribution, with respect to the CONKEMO results, for V13 at 0 and 60 MWd/kg are shown in Figs. 11 and 12, respectively and for V14 at 0 and 60 MWd/kg in Figs. 13 and 14, respectively. The results show excellent agreement with the average difference of approximately 1% and the maximum differences of about 5%. This indicates that the codes agree reasonably well even with the large power peaking that occurs at the UO_2/MOX interface in the uniform MOX assembly variant (V13) at 0 MWd/kg.

4.4 KINETICS PARAMETERS

For variants V15-V20 kinetics parameters were also calculated. The effective delayed neutron fractions are presented in Table 6 and the prompt neutron lifetimes are given in Table 7. The values agree extremely well across all of the variants and states.

5. CONCLUSIONS

Variants of pin cell, assembly, and multi-assembly VVER-1000 structures have been computed with several different codes used in the U.S. and Russia. A comparison of results shows good agreement among the various codes. Discrepancies were noted in an extreme pin cell case that contains only 241Pu and are attributed to different data and resonance treatment of this isotope. The trends of k_{eff} versus burnup were slightly different for the MOX cases resulting in differences of over 1% at a burnup of 60 MWd/kg. The single assembly and multi-assembly calculations show very good agreement, particularly in the calculated power distributions. The calculation of kinetics parameters shows excellent agreement as well.

As a result of this benchmarking activity the level of agreement between the U.S. and Russian methods have been established and found to be reasonable for design analyses. Similar methods and models are now being used to design lead test assemblies and mission fuel assemblies. In the future, benchmarking efforts will be extended to the whole-core methods involving fuel cycle and kinetics calculations.

REFERENCES

1. A. G. Kalashnikov, et al., "Calculation of VVER Reactor Computational Benchmark Pin Cell Variants," *Trans. Am. Nuc. Soc.,* **79**, 294 (1998).
2. M. A. Kalugin, et al., "Computational Benchmarks for LEU and MOX Fuel in VVER Reactors," *Trans. Am. Nuc. Soc.,* **79**, 290 (1998).
3. A. P. Lazarenko, et al., "Calculation of the Weapons-Grade MOX VVER Assembly Benchmarks," *Trans. Am. Nuc. Soc,* **79**, 292 (1998).
4. R. T. Primm, *Neutronics Benchmarks for the Utilization of MOX Fuel: Joint U.S./Russian Progress Report for Fiscal Year 1997*, ORNL/TM-13603, Vol. 3, Oak Ridge National Laboratory (1998).
5. P. Lazarenko, Russian Research Center, Kurchatov Institute, Personal Communication (Sept. 1997).
6. J. C. Gehin, et al., *Analysis of Weapons-Grade MOX VVER-1000 Benchmarks with HELIOS and KENO,* ORNL/TM-1999/78, Oak Ridge National Laboratory (July 1999)
7. E. Gomin and L. Maiorov, "The MCU-RFFI Code," *Proceedings of the Int. Conf. on Math., Comp. Reactor Phys. and Envir.*, Portland, Oregon, Apr. 30-May 4, 1995.
8. *SCALE: A Modular Code System for Performing Standardized Computer Analysis for Licensing Evaluations*, NUREG/CR-200, Rev. 4 (ORNL/NUREG/CSD-2R4), Vols I, II, and III, Oak Ridge National Laboratory (April 1995).
9. Manturov G.N., Nikolaev M.N., Tsibulya A.M., *System of group constants ABBN-93. Verification Report 1, Recommended Reference Data*, Moscow 1995
10. V. D. Sidorenko et al., "Spectral Code TVS-M for Calculation of Characteristics of Cells, Supercells and Fuel Assemblies of VVER-Type Reactors," *Fifth Symposium of the AER*, Dobogoko, Hungary, October 15-20, 1995.
11. J. R. Askew, et al., "A General Description of the Lattice Code WIMS," *Journal of the British Nuclear Energy Society*, **5** (1), 564-584 (1966).
12. J. J. Casal, et al., "HELIOS: Geometric Capabilities of a New Fuel-Assembly Program," *Proceedings International Topical Meeting Advances in Mathematics, Computation, and Reactor Physics*, April 28-May 2, 1991, 10.21-1.
13. D. R. Vondy, et al., *The BOLD VENTURE Computation System for Nuclear Reactor Core Analysis, Version III,* ORNL-5711, Union Carbide Corp., Oak Ridge National Laboratory (June 1981).
14. R. J. Ellis, *Analysis of Weapons-Grade MOX VVER-1000 Neutronics Benchmarks: Pin-Cell Calculations with SCALE/SAS2H,* ORNL/TM-2000/4, Oak Ridge National Laboratory (Jan. 2000).

Table 1. Specification of Benchmark Fuel Variants

Variant	Description	Variant	Description
V1	UO_2 pin cell	V12	WG MOX Assembly
V2	MOX pin cell	V13	Multi-assembly with uniform MOX assembly
V3	Spent UO_2 pin cell, no fission products	V14	Multi-assembly with graded MOX assembly
V4	Spent UO_2 pin cell, with fission products	V15	UO_2 pin cell, accident conditions, kinetics parameters
V7	MOX pin cell with ^{239}Pu only	V16	Spent UO_2 pin cell, accident conditions, kinetics parameters S1, S3–S6
V8	MOX pin cell with ^{240}Pu only	V17	MOX pin cell, accident conditions, kinetics parameters S1, S3–S6
V9	MOX pin cell with ^{241}Pu only	V18	Spent MOX pin cell, accident conditions, kinetics parameters S1, S3–S6
V10	Reactor MOX pin cell	V19	Multi-assembly, accident conditions, kinetics parameters
V11	UO_2 Assembly	V20	Multi-assembly with spent UO_2 assemblies, accident conditions, kinetics parameters

Table 2. Calculational States

State	Fuel temp. (K)	Non-fuel temp.(K)	Moderator material[a]	Control Rods	^{135}Xe and ^{149}Sm fission products	Buckling (cm^{-2})
S1	1027	579	MOD1	none	present	0.003
S2	1027	579	MOD1	present	present	0.003
S3	1027	579	MOD2	none	none	0.003
S4	1027	579	MOD1	none	present	0.003
S5	579	579	MOD1	none	none	0.003
S6	300	300	MOD3	none	none	0.003
S7	1027	579	MOD2	none	none	0.0
S8	2000	579	MOD2	none	none	0.0
S9	1027	579	MOD4	none	none	0.0
S10	1027	579	MOD6	none	none	0.0
S11	1027	579	MOD2	none	none	Critical
S12	300	300	MOD5	none	none	Critical

[a]Moderator descriptions:

MOD1	Hot moderator with 600 ppm boron
MOD2	Hot moderator without boron
MOD3	Cold moderator with 600 ppm boron
MOD4	Hot moderator of low density
MOD5	Cold moderator without boron
MOD6	Hot moderator with 1200 ppm boron

Table 3. Comparison of Pin Cell Variant k_{eff} Values at 0 MWd/kg

		k_{eff}				Percent Difference from TVS-M[a]		
		TVS-M	**MCU**	**WIMS-ABBN**	**HELIOS**	**MCU**	**WIMS-ABBN**	**HELIOS**
V1	S1	1.0617	1.0639	1.0572	1.0648	0.21	-0.42	0.29
	S3	1.1073	-	1.1024	1.1110	-	-0.44	0.33
	S4	1.1028	1.1033	1.0962	1.1039	0.05	-0.60	0.10
	S5	1.1159	1.1161	1.1109	1.1173	0.02	-0.46	0.12
	S6	1.2200	1.2187	1.2160	1.2207	-0.11	-0.33	0.06
V2	S1	1.0233	1.0200	1.0149	1.0227	-0.33	-0.83	-0.06
	S3	1.0477	-	1.0385	1.0469	-	-0.88	-0.08
	S4	1.0412	1.0368	1.0310	1.0389	-0.43	-0.98	-0.22
	S5	1.0569	1.0498	1.0483	1.0551	-0.67	-0.81	-0.17
	S6	1.1818	1.1786	1.1779	1.1832	-0.27	-0.34	0.12
V3	S1	0.9127	-	0.9136	0.9128	-	0.10	0.01
	S3	0.9502	-	0.9506	0.9500	-	0.05	-0.02
	S4	0.9477	-	0.9465	0.9453	-	-0.13	-0.25
	S5	0.9621	-	0.9615	0.9604	-	-0.06	-0.17
	S6	1.0610	1.0574	1.0619	1.0603	-0.34	0.09	-0.07
V4	S1	0.8569	-	0.8598	0.8602	-	0.34	0.38
	S3	0.8905	0.8915	0.8931	0.8936	0.12	0.30	0.35
	S4	0.8879	0.8883	0.8890	0.8890	0.05	0.13	0.13
	S5	0.9010	0.9002	0.9025	0.9029	-0.09	0.17	0.22
	S6	0.9982	0.9984	1.0007	1.0005	0.02	0.25	0.23
V7	S1	1.0965	-	1.0967	1.1046	-	0.02	0.74
	S3	1.1240	-	1.1237	1.1321	-	-0.03	0.72
	S4	1.1166	-	1.1151	1.1229	-	-0.14	0.56
	S5	1.1303	-	1.1303	1.1369	-	-0.01	0.58
	S6	1.2509	1.2501	1.2542	1.2595	-0.06	0.27	0.69
V8	S1	0.9281	-	0.9160	0.9240	-	-1.30	-0.44
	S3	0.9731	-	0.9599	0.9690	-	-1.35	-0.42
	S4	0.9711	-	0.9563	0.9646	-	-1.52	-0.67
	S5	0.9856	-	0.9728	0.9800	-	-1.29	-0.57
	S6	1.0881	1.0828	1.0780	1.0831	-0.49	-0.93	-0.46
V9	S1	1.2797	-	1.3247	1.3228	-	3.52	3.37
	S3	1.3096	-	1.3552	1.3543	-	3.48	3.41
	S4	1.3001	-	1.3443	1.3425	-	3.40	3.26
	S5	1.3167	-	1.3611	1.3593	-	3.37	3.24
	S6	1.4337	1.4372	1.4747	1.4713	0.24	2.85	2.62
V10	S1	0.9648	-	0.9517	0.9593	-	-1.36	-0.57
	S3	0.9762	-	0.9629	0.9707	-	-1.35	-0.56
	S4	0.9704	-	0.9566	0.9643	-	-1.42	-0.63
	S5	0.9848	-	0.9716	0.9799	-	-1.34	-0.50
	S6	1.0942	-	1.0851	1.0910	-	-0.83	-0.29

[a] $(x - \text{TVS-M})/\text{TVS-M} \times 100$

Table 4. Comparison of Assembly Variant k_{eff} Values at 0 and 60 MWd/kg

Variant Burnup		k_{eff}			Percent Difference from TVS-M	
		TVS-M	WIMS-ABBN	HELIOS	WIMS-ABBN	HELIOS
V11 0 MWd/kg	S1	1.0757	1.0673	1.0791	-0.78	0.32
	S2	0.8416	0.8361	0.8412	-0.64	-0.04
	S3	1.1313	1.1221	1.1351	-0.81	0.34
	S4	1.1189	1.1085	1.1203	-0.93	0.12
	S5	1.1307	1.1226	1.1326	-0.72	0.16
	S6	1.2197	1.2156	1.2226	-0.34	0.24
V11 60 MWd/kg	S1	0.6993	0.7066	0.7027	1.04	0.49
	S2	0.5463	0.5472	0.5485	0.17	0.41
	S3	0.7387	0.7441	0.7421	0.73	0.46
	S4	0.7212	0.7313	0.7277	1.40	0.90
	S5	0.7313	0.7415	0.7383	1.40	0.96
	S6	0.7777	0.7934	0.7831	2.02	0.70
V12 0 MWd/kg	S1	1.0486	1.0367	1.0483	-1.13	-0.03
	S2	0.8570	0.8537	0.8568	-0.39	-0.03
	S3	1.0795	1.0665	1.0788	-1.21	-0.06
	S4	1.0683	1.0551	1.0663	-1.24	-0.19
	S5	1.0826	1.0718	1.0812	-1.00	-0.13
	S6	1.1956	1.1927	1.1995	-0.24	0.32
V12 60 MWd/kg	S1	0.6861	0.6953	0.6962	1.35	1.48
	S2	0.5439	0.5522	0.5515	1.53	1.40
	S3	0.7194	0.7268	0.7295	1.03	1.41
	S4	0.7070	0.7188	0.7200	1.67	1.84
	S5	0.7170	0.7289	0.7311	1.67	1.97
	S6	0.7644	0.7835	0.7775	2.50	1.71

Table 5. Calculated Control Rod Worths for Variants V11 and V12 at 0 and 60 MWd/kgHM

Variant	Burnup (MWd/kgHM)	Control Rod Worth (% reactivty)		
		TVS-M	WIMS-ABBN	HELIOS
V11	0	-25.9	-25.9	-26.2
V11	60	-40.0	-41.2	-40.0
V12	0	-21.3	-20.7	-21.3
V12	60	-38.1	-37.3	-37.7

Table 6. Effective Delayed Neutron Fractions for Benchmark Variants V15-V20.

Variant	State	MCU-RFFI/A	TVS-M	WIMS-ABBN/ TRIANG	HELIOS
V15	S7	7.130E-03	7.202E-03	7.161E-03	7.192E-03
	S8	7.120E-03	7.203E-03	7.161E-03	7.194E-03
	S9	7.330E-03	7.392E-03	7.369E-03	7.500E-03
	S10	7.120E-03	7.203E-03	7.164E-03	7.202E-03
	S11	-	8.218E-03	8.143E-03	8.225E-03
	S12	-	8.404E-03	8.312E-03	8.354E-03
V16	S7	5.150E-03	5.309E-03	5.211E-03	5.289E-03
	S8	-	5.318E-03	5.200E-03	5.276E-03
	S9	-	5.949E-03	5.879E-03	6.061E-03
	S10	5.170E-03	5.328E-03	5.232E-03	5.317E-03
	S11	-	5.559E-03	5.454E-03	5.558E-03
	S12	-	5.853E-03	5.755E-03	5.846E-03
V17	S7	3.140E-03	3.170E-03	3.169E-03	3.231E-03
	S8	3.170E-03	3.184E-03	3.184E-03	3.248E-03
	S9	3.890E-03	3.962E-03	3.977E-03	4.160E-03
	S10	3.170E-03	3.200E-03	3.200E-03	3.266E-03
	S11	-	3.576E-03	3.550E-03	3.657E-03
	S12	-	3.542E-03	3.511E-03	3.583E-03
V18	S7	3.730E-03	3.874E-03	3.752E-03	3.896E-03
	S8	-	3.890E-03	3.761E-03	3.908E-03
	S9	-	4.764E-03	4.642E-03	4.880E-03
	S10	3.750E-03	3.912E-03	3.789E-03	3.938E-03
	S11	-	4.023E-03	3.891E-03	4.055E-03
	S12	-	4.035E-03	3.901E-03	4.046E-03
V19	S7	6.140E-03	6.071E-03	6.326E-03	6.172E-03
	S8	-	6.076E-03	6.325E-03	6.179E-03
	S9	-	6.333E-03	6.610E-03	6.596E-03
	S10	-	6.066E-03	6.286E-03	6.161E-03
	S11	-	6.926E-03	7.144E-03	7.083E-03
	S12	-	7.093E-03	7.270E-03	7.191E-03
V20	S7	4.530E-03	4.603E-03	4.560E-03	4.650E-03
	S8	-	4.611E-03	4.334E-03	4.645E-03
	S9	-	5.236E-03	5.321E-03	5.453E-03
	S10	-	4.620E-03	4.564E-03	4.667E-03
	S11	-	4.943E-03	4.934E-03	5.027E-03
	S12	-	5.167E-03	5.060E-03	5.198E-03

Table 7. Prompt Neutron Lifetime (s) for Benchmark Variants V15-V20

Variant	State	TVS-M	WIMS-ABBN/ TRIANG	HELIOS
V15	S7	2.109E-05	2.110E-05	2.111E-05
	S8	2.101E-05	2.110E-05	2.106E-05
	S9	1.604E-05	1.600E-05	1.591E-05
	S10	1.877E-05	1.880E-05	1.881E-05
	S11	2.047E-05	2.040E-05	2.035E-05
	S12	2.106E-05	2.120E-05	2.089E-05
V16	S7	1.945E-05	1.920E-05	1.909E-05
	S8	1.936E-05	1.900E-05	1.876E-05
	S9	1.290E-05	1.580E-05	1.253E-05
	S10	1.719E-05	1.700E-05	1.692E-05
	S11	1.926E-05	1.900E-05	1.888E-05
	S12	2.177E-05	2.190E-05	2.159E-05
V17	S7	1.118E-05	1.080E-05	1.088E-05
	S8	1.109E-05	1.070E-05	1.057E-05
	S9	8.639E-06	8.300E-06	8.483E-06
	S10	1.034E-05	1.010E-05	1.011E-05
	S11	1.098E-05	1.060E-05	1.065E-05
	S12	1.321E-05	1.310E-05	1.303E-05
V18	S7	1.470E-05	1.430E-05	1.427E-05
	S8	1.460E-05	1.410E-05	1.388E-05
	S9	9.847E-06	9.400E-06	9.493E-06
	S10	1.325E-05	1.290E-05	1.292E-05
	S11	1.460E-05	1.420E-05	1.417E-05
	S12	1.757E-05	1.750E-05	1.739E-05
V19	S7	1.491E-05	-	1.943E-05
	S8	1.516E-05	-	1.933E-05
	S9	1.434E-05	-	1.486E-05
	S10	1.443E-05	-	1.726E-05
	S11	1.985E-05	-	1.878E-05
	S12	2.133E-05	-	1.987E-05
V20	S7	1.626E-05	-	1.772E-05
	S8	1.657E-05	-	1.742E-05
	S9	1.520E-05	-	1.239E-05
	S10	1.557E-05	-	1.570E-05
	S11	1.875E-05	-	1.744E-05
	S12	2.171E-05	-	2.010E-05

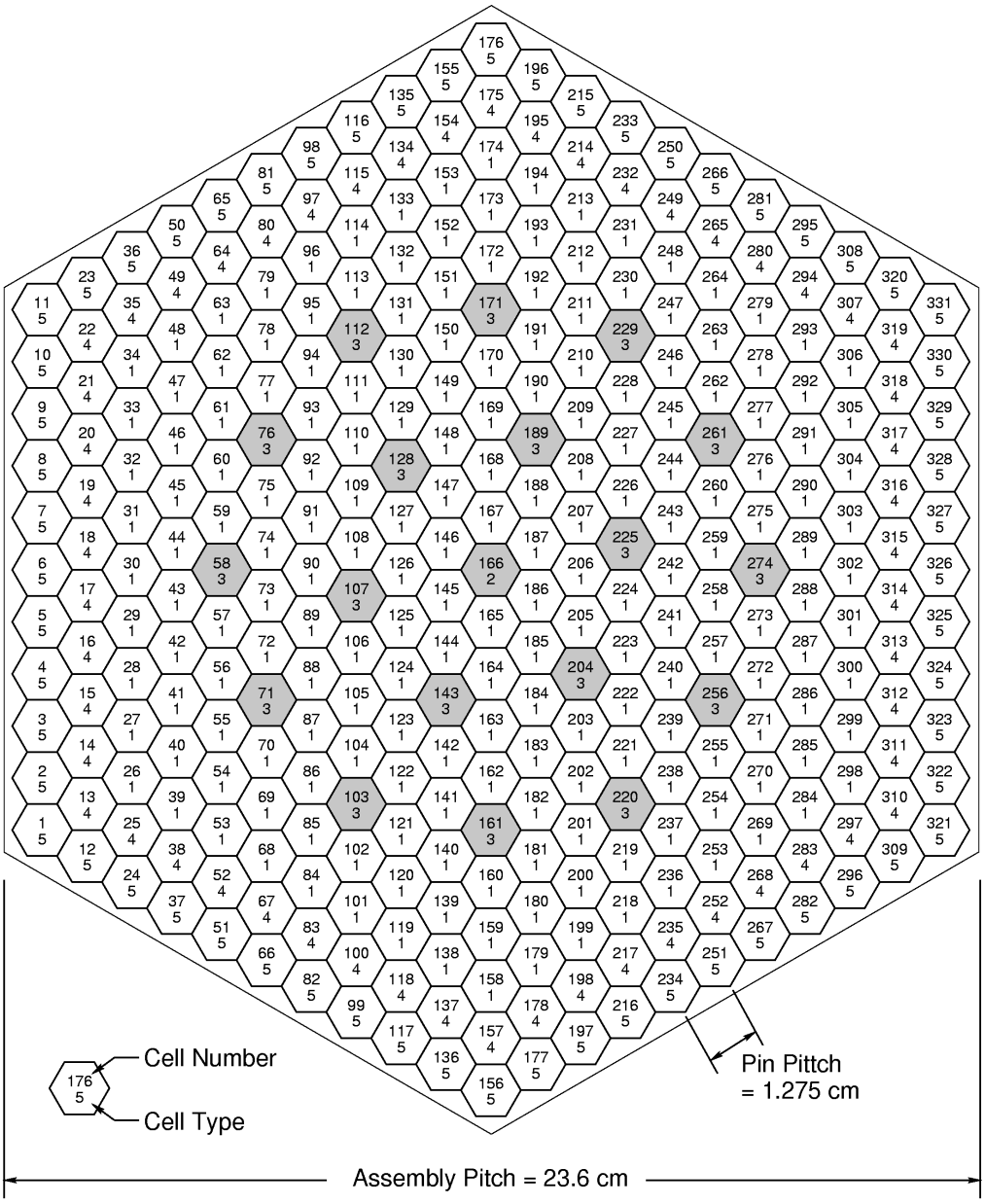

Fig. 1 VVER-1000 assembly

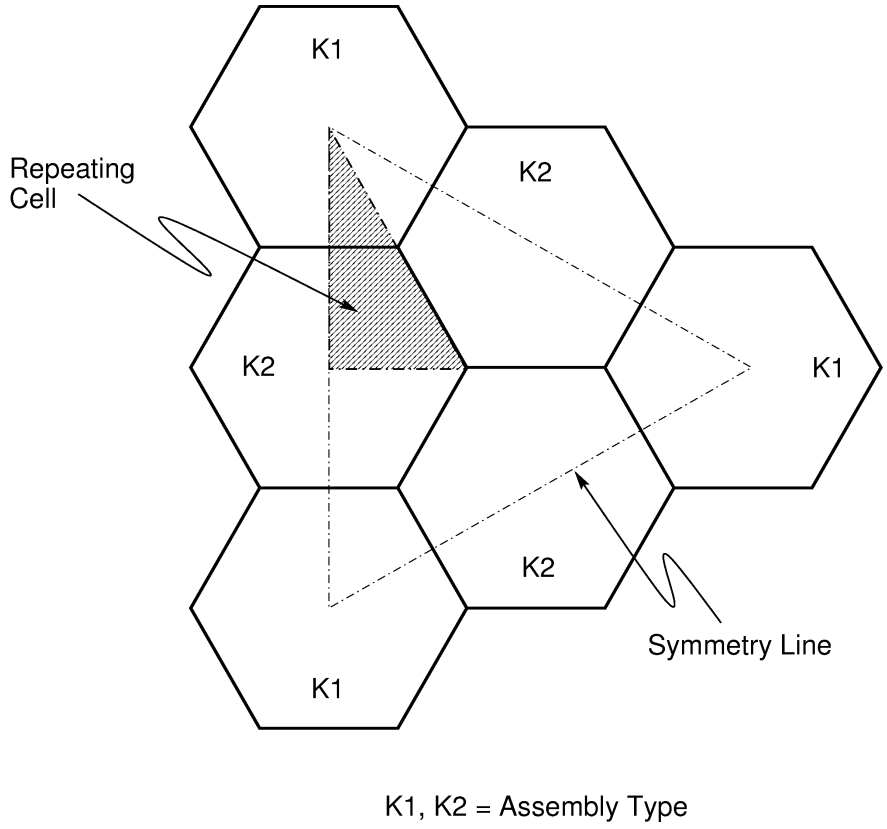

Fig.2 Multi-assembly structure (K1=MOX, K2=UO_2)

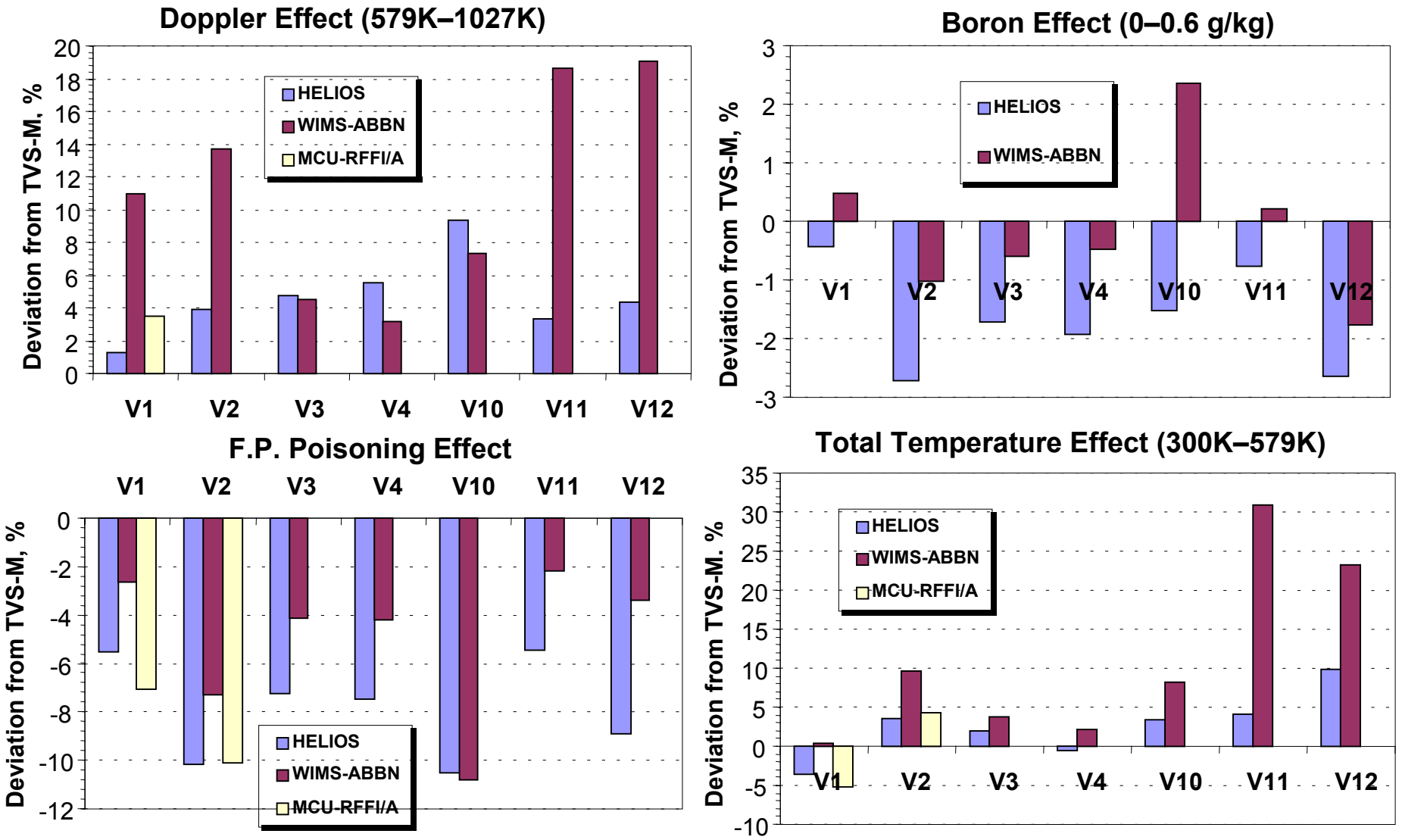

Fig. 3 Comparison of the reactivity effects for pin cell variants V1-V4, V10 and assembly variants V11 and V12.

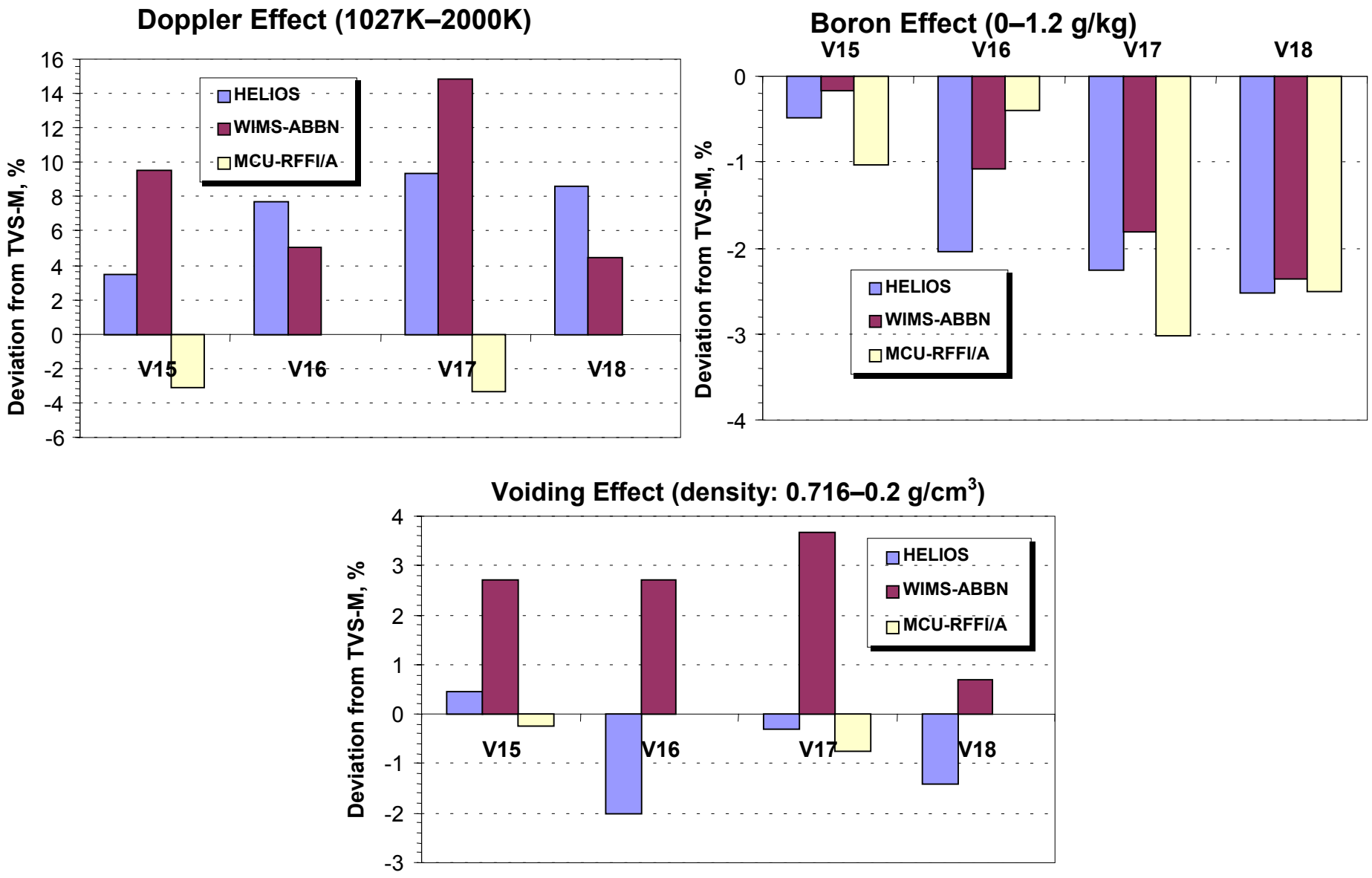

Fig. 4 Comparison of the reactivity effects for pin cell variants V15-V18.

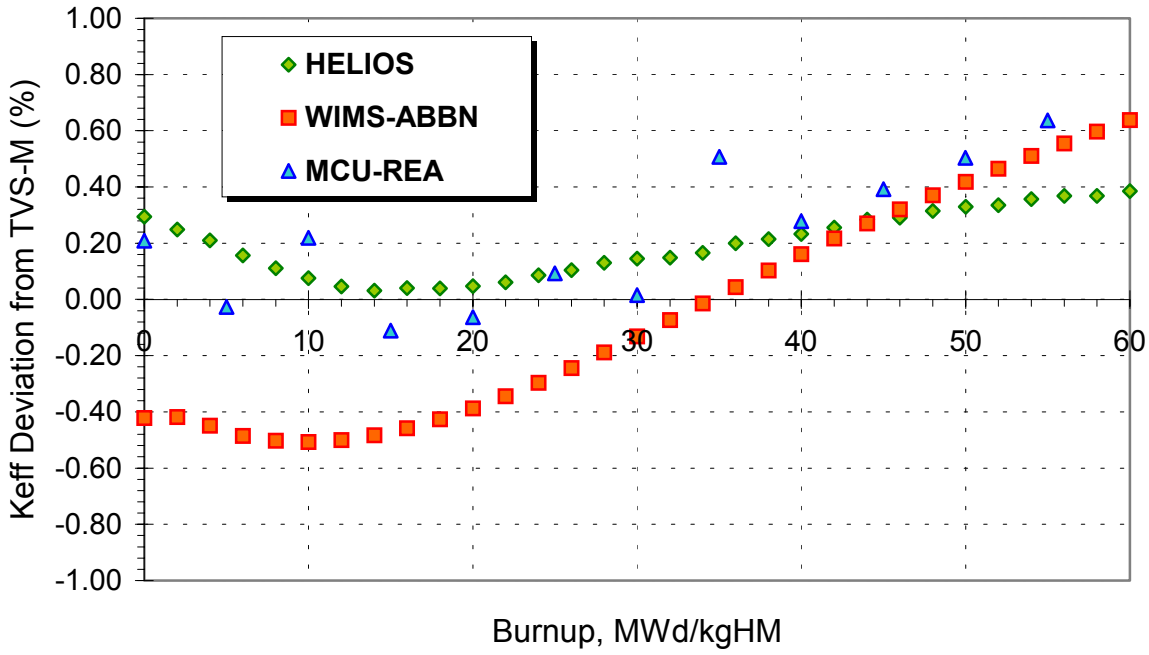

Fig. 5 Comparison of k_{eff} (percent difference from TVS-M) versus burnup for benchmark variant V1

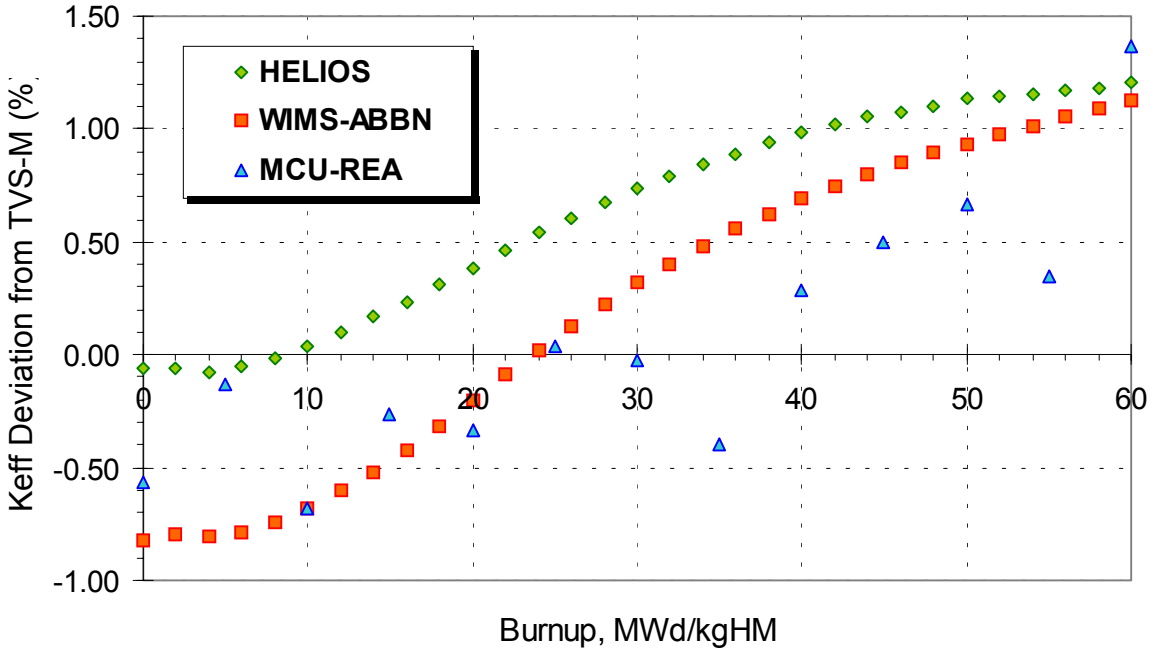

Fig. 6 Comparison of k_{eff} (percent difference from TVS-M) versus burnup for benchmark variant V2

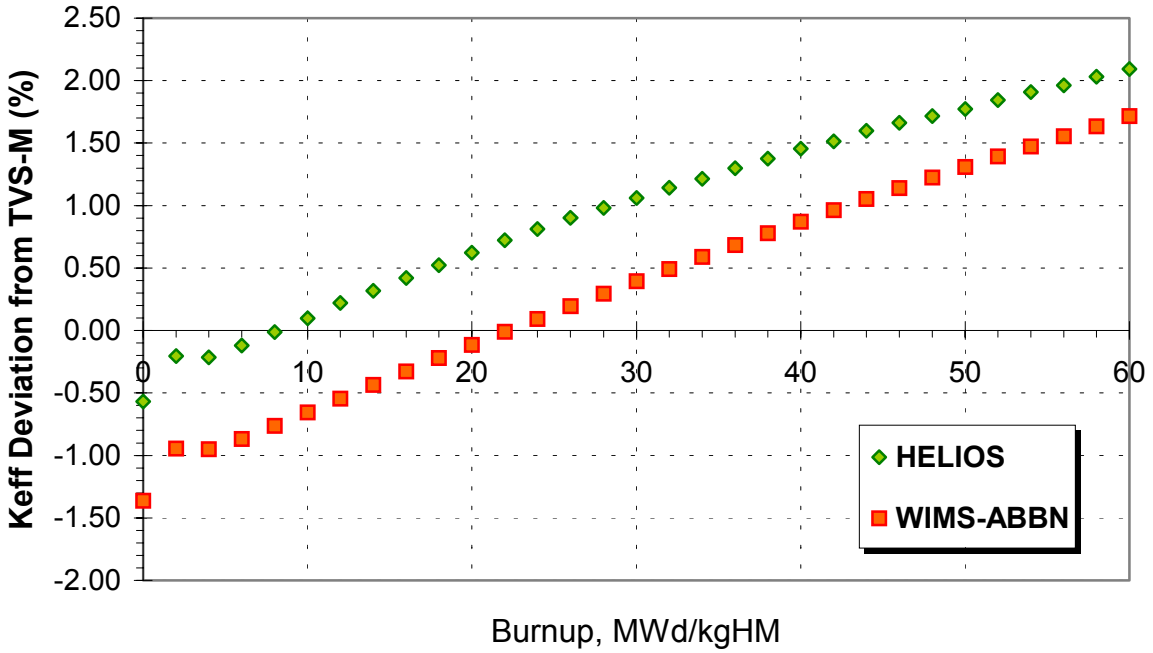

Fig. 7 Comparison of k_{eff} (percent difference from TVS-M) versus burnup for benchmark variant V10

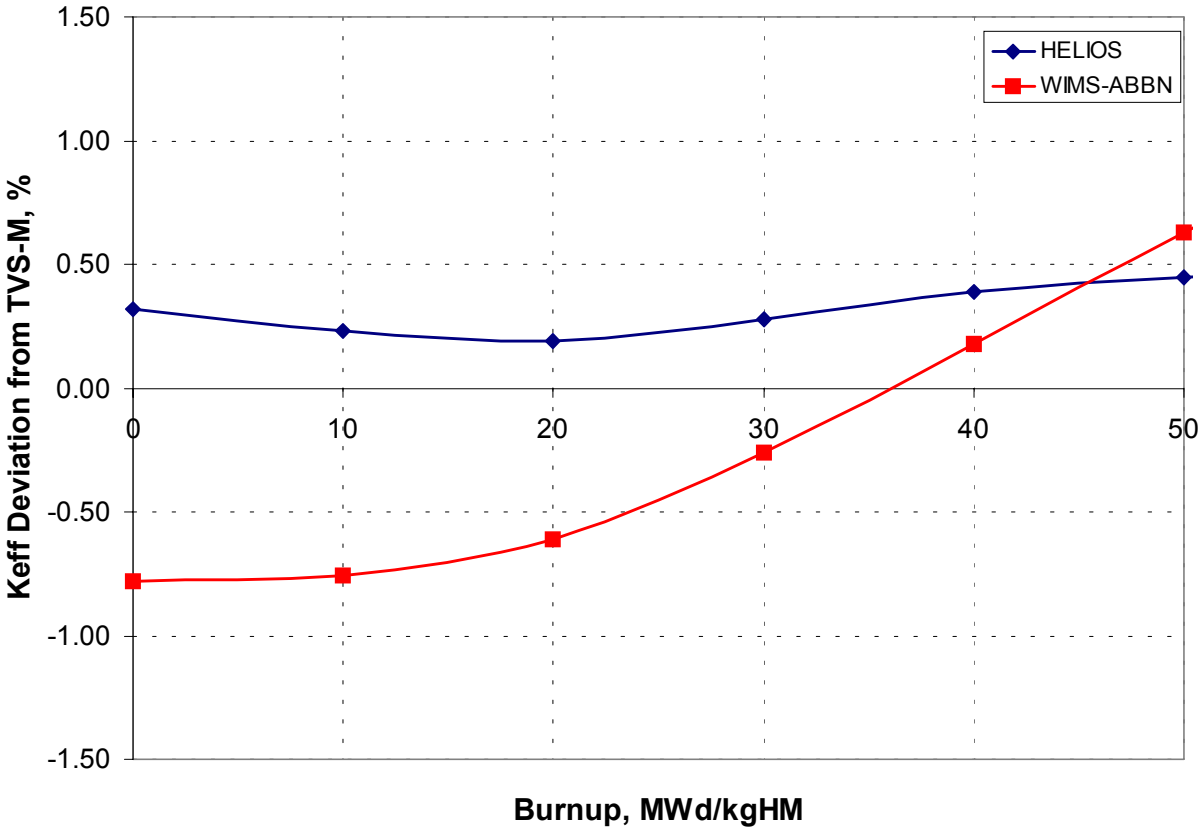

Fig. 8 Comparison of k_{eff} (percent difference from TVS-M) versus burnup for benchmark variant V11

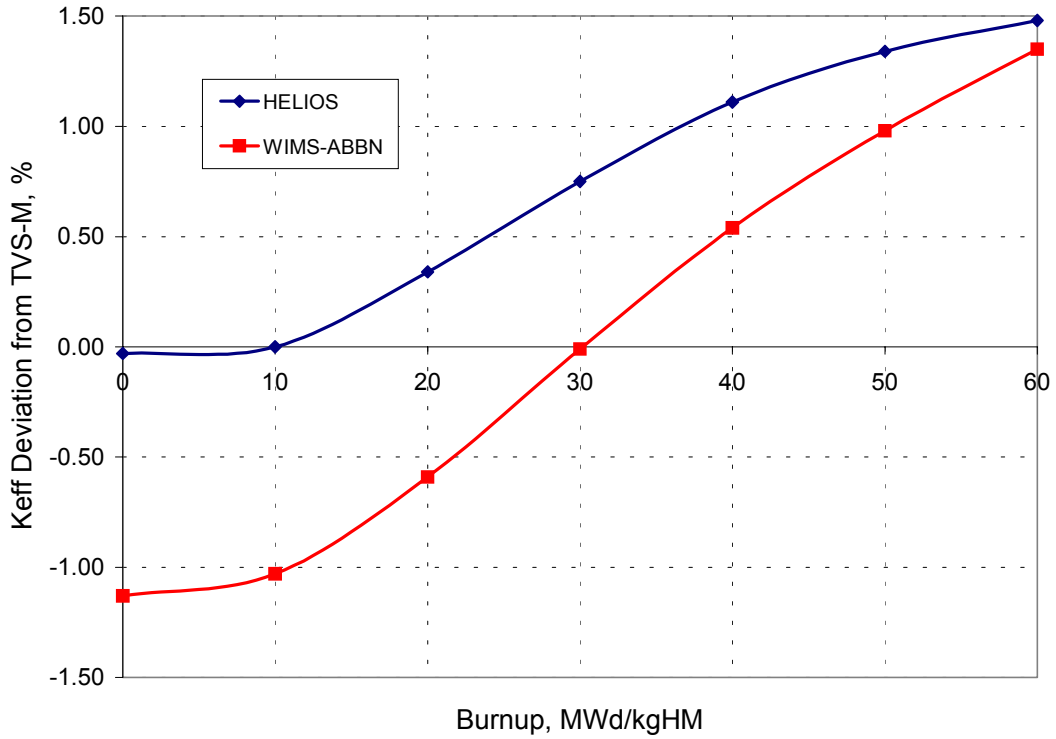

Fig. 9 Comparison of k_{eff} (percent difference from TVS-M) versus burnup for benchmark variant V12

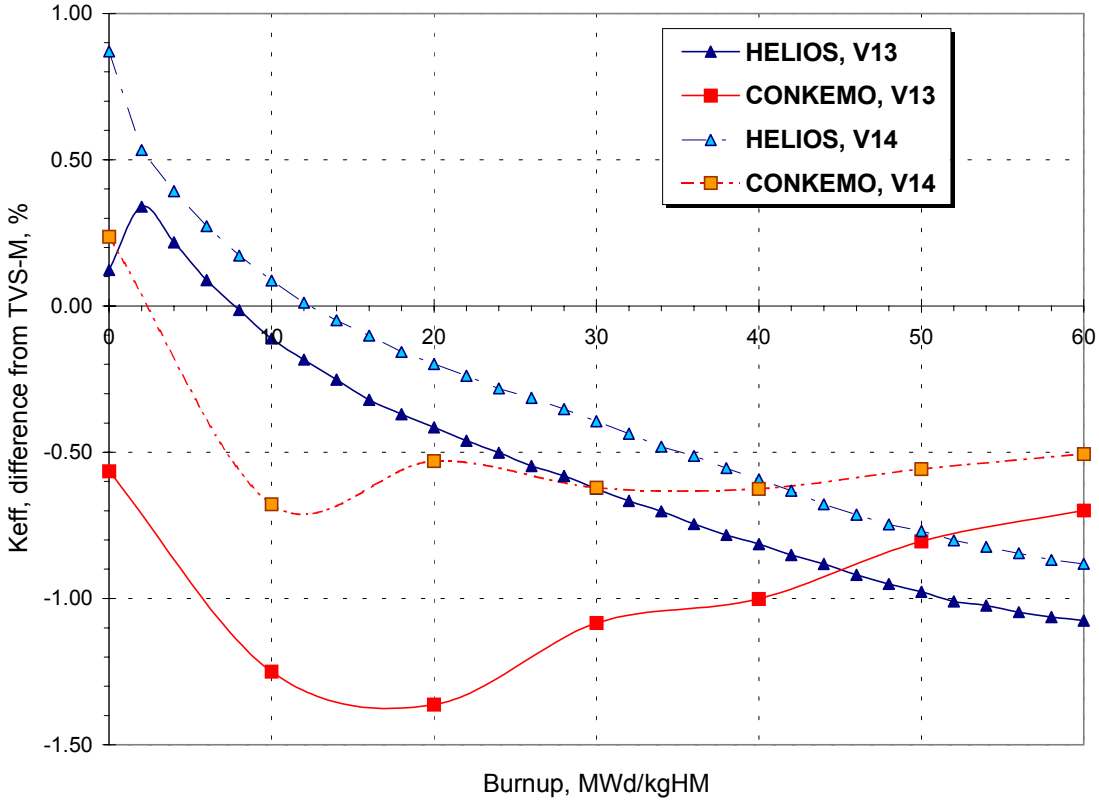

Fig. 10 Comparison of k_{eff} (percent difference from TVS-M) versus burnup for benchmark variants V13 and V14

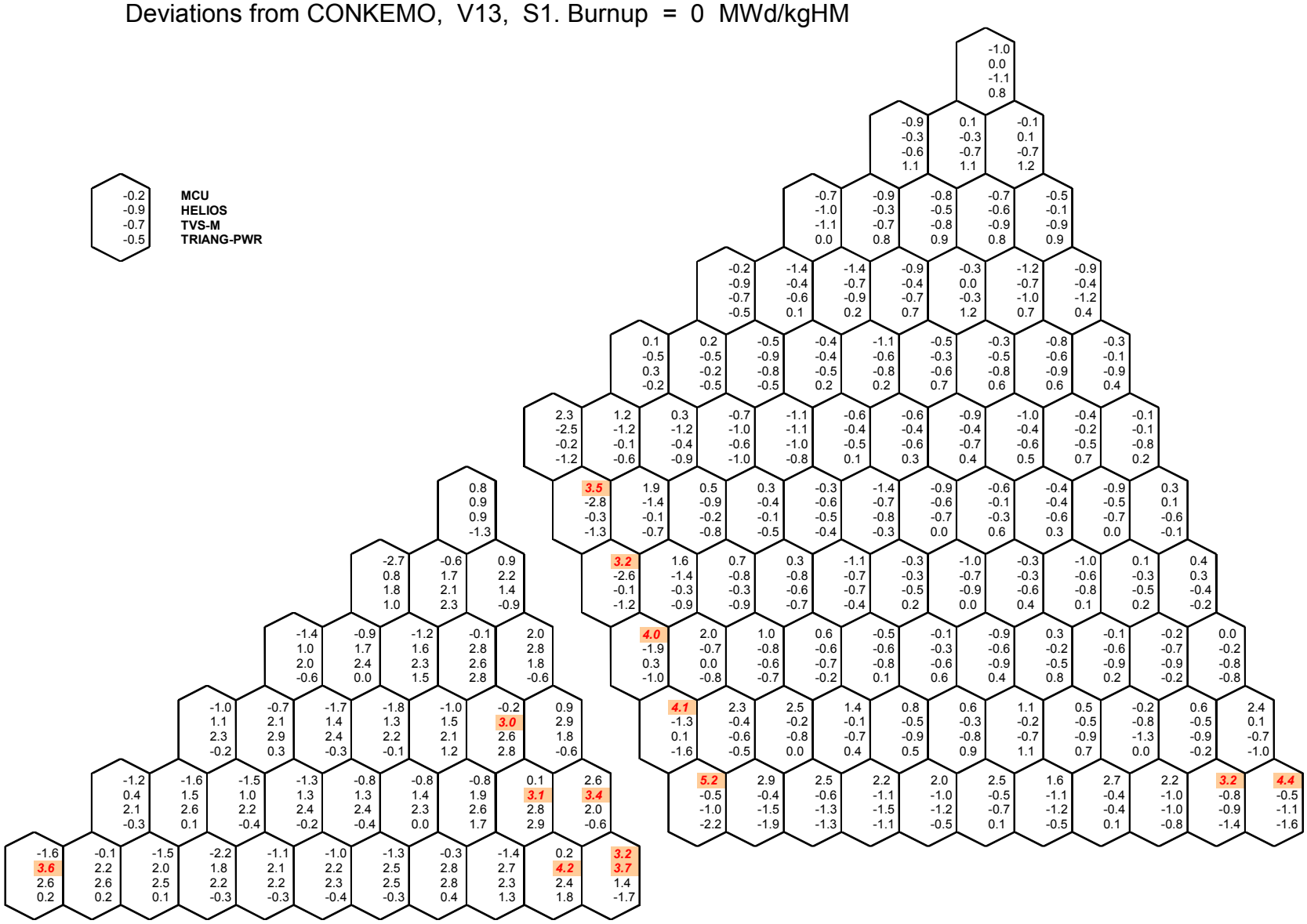

Fig. 11 Comparison of pin power density (relative to CONKEMO results) for variant V13 at 0 MWd/kgHM

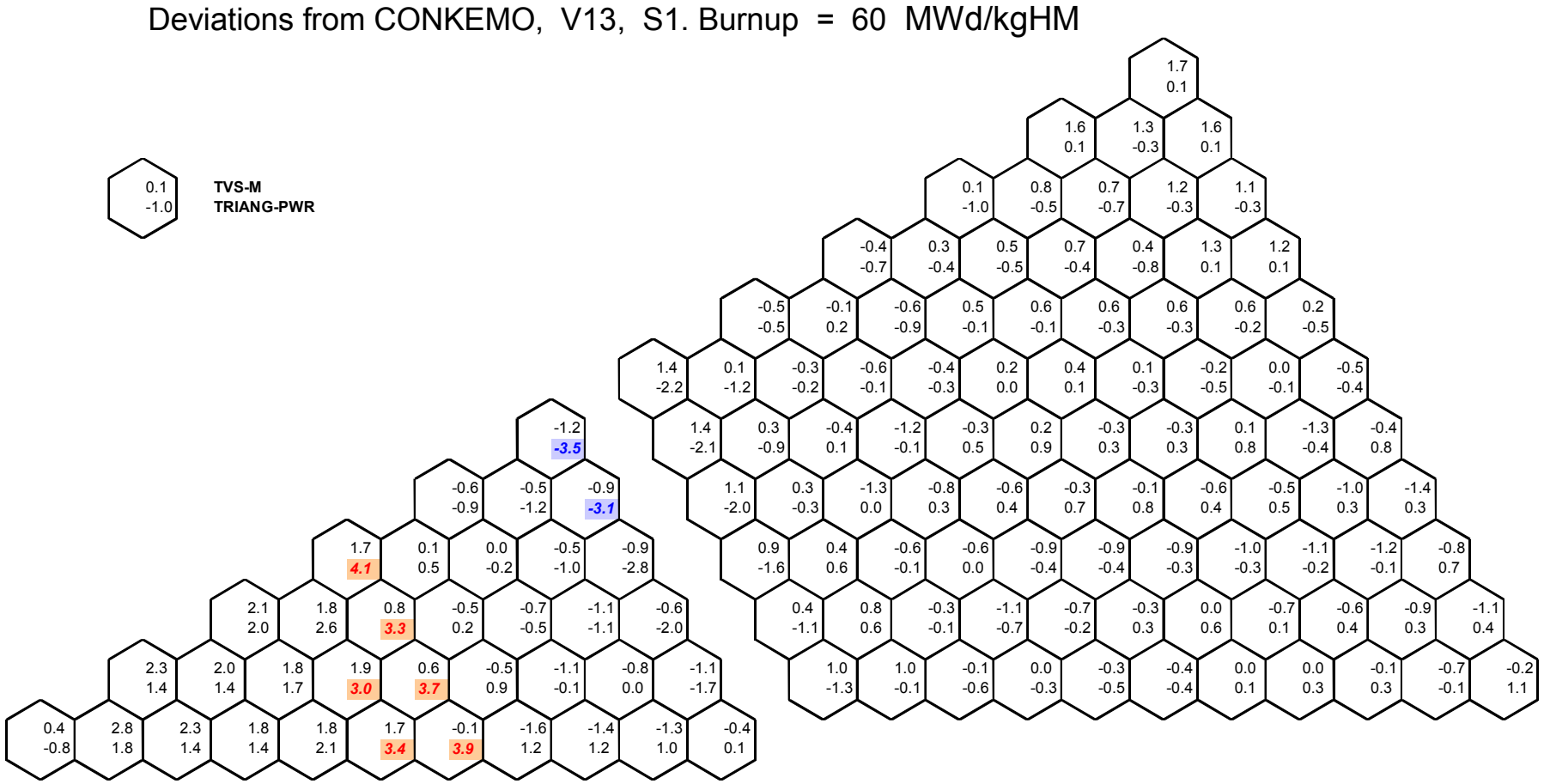

Fig. 12 Comparison of pin power density (relative to CONKEMO results) for variant V13 at 60 MWd/kgHM

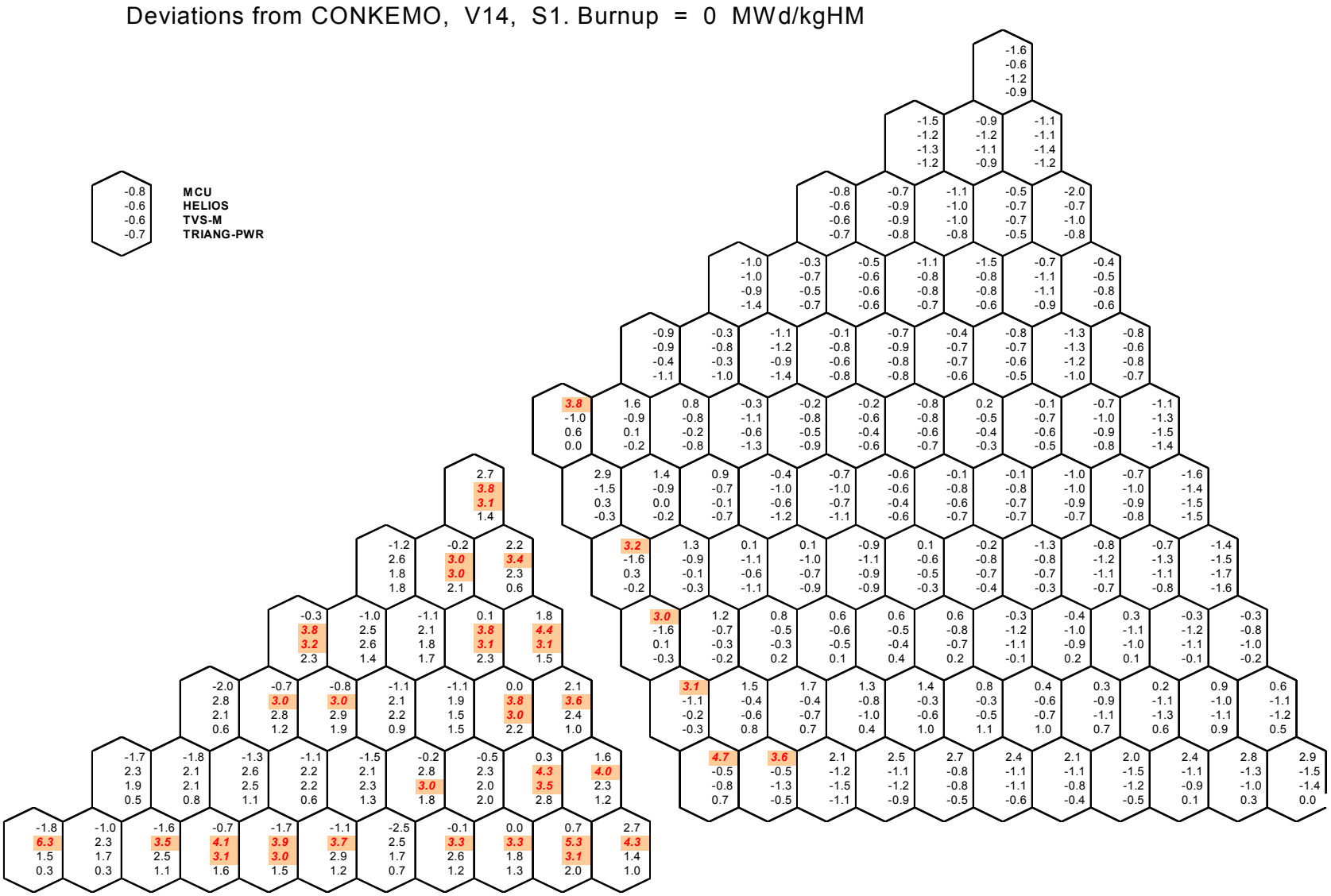

Fig. 13 Comparison of pin power density (relative to CONKEMO results) for variant V14 at 0 MWd/kgHM

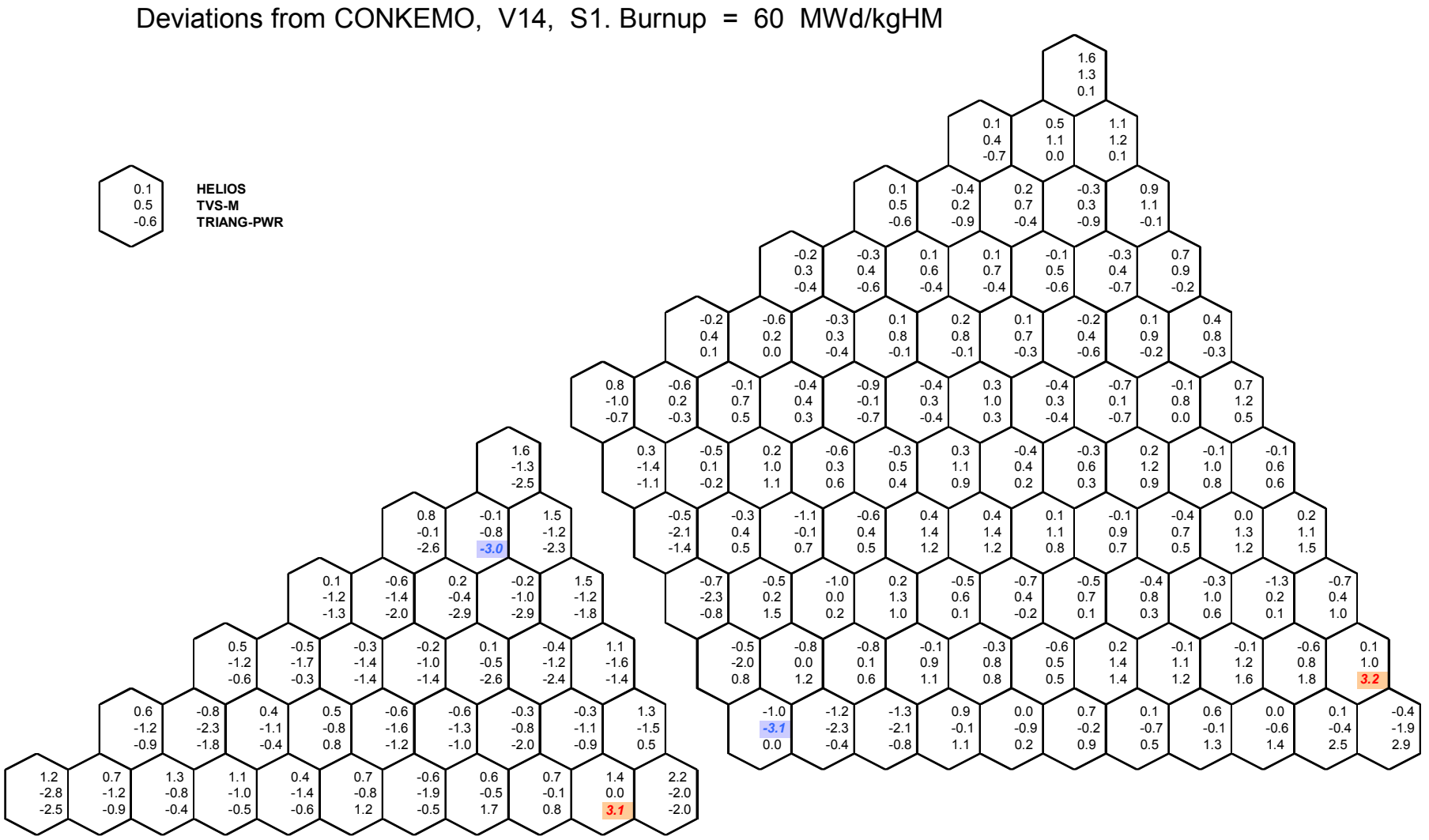

Fig. 14 Comparison of pin power density (relative to CONKEMO results) for variant V14 at 60 MWd/kgHM